



## Spark Plasma Sintering of Ultra-high Temperature Tantalum/Hafnium Carbides Composite

F. Arianpour\*, F. Golestanifard, H.R. Rezaie

School of Metallurgy and Materials Engineering, Iran University of Science and Technology, Narmak, 16844, Tehran, Iran.

### PAPER INFO

#### Paper history:

Received 14 November 2015

Accepted in revised form 16 February 2016

#### Keywords:

Tantalum carbide

Carbon nanotubes

Sintering

Mechanical properties

Phase evolution.

### ABSTRACT

TaC and HfC are thought to have the highest melting point among all refractory materials. The binary solid solution of TaC and HfC is also considered as the most refractory material with melting points over 4000 °C and valuable physical and mechanical properties. The main goal of this work is to fabricate TaC/HfC based composites which consolidated by means of spark plasma sintering with addition of MoSi<sub>2</sub> as sintering aid and carbon nanotubes as reinforcement at 2000 °C. The effects of additives were investigated in terms of densification, mechanical properties, phase and microstructural evolutions. It was demonstrated that the relative density could reach near 99 % for samples containing additives, from 94 % TD for sample without sintering aid respectively. The average Vickers hardness and fracture toughness values were in the range of 16-19 MPa and 2.9-5.3 MPa.m<sup>1/2</sup>. The samples containing CNTs showed improved fracture toughness and the survivability of CNTs, after spark plasma sintering, was proved by scanning electron microscopy of fractured surfaces in addition to the Raman spectroscopy analysis.

## 1. INTRODUCTION

Ultra high temperature ceramics (UHTCs) offer excellent stability at temperatures exceeding 2000 °C being investigated as possible thermal protection systems (TPS), coatings subjected to high temperatures, and bulk materials for heating elements [1,2]. Basically, UHTCs are classified in borides, carbides and nitrides of transition metals. Current efforts have focused on heavy, transition metal carbides and borides such as TaC, HfC, HfB<sub>2</sub>, TaB<sub>2</sub> and their associated composites [2]. These materials all exhibit strong covalent bonding which gives them structural stability at high temperatures. Carbides are essentially brittle due to the strong bonds that exist between carbon atoms. The largest class of carbides, including Hf, Zr, Ti and Ta carbides have high melting points due to covalent carbon networks although carbon vacancies often exist in these materials; indeed, TaC and HfC have the highest melting points rather than any other materials [3]. The crystal structures, lattice parameters, densities, and melting points of some UHTCs are shown in Table 1. It is extremely important that UHTCs have the ability to retain high bending

strength and hardness at high temperatures (above 2000 °C). UHTCs generally exhibit hardness above 20 GPa due to the strong covalent bonds existed in these materials. However, different methods of processing can lead to great variation in mechanical values [4-6]. It has been shown that UHTC ceramics synthesized as a composite with carbon nanotubes (CNTs) exhibit increasing in fracture toughness relative to the pure materials. This is due to material densification and a reduction in grain size upon processing [7,8]. UHTCs often require high temperature and pressure processing to produce dense and durable materials. The high melting points and strong covalent interactions make them difficult to achieve uniform densification. Densification is only achieved at temperatures above 1800 °C once grain boundary diffusion mechanisms become active. Unfortunately, processing of UHTCs at these temperatures results in materials with larger grain sizes and poor mechanical properties [9,10].

Some additives such as metal di-silicide can be used in order to form a liquid phase during sintering. It should be noted that these additives may reduce the maximum temperature at which UHTCs can operate due to the formation of eutectic liquids [11,12]. Hot pressing is a popular method for obtaining densified materials that

\*Corresponding Author's Email: [arianpour@iust.ac.ir](mailto:arianpour@iust.ac.ir)

relies upon both high temperatures and pressures. Hot pressing temperature, pressure, heating rate, reaction atmosphere, and holding times are all factors that affect the density and microstructure. In order to achieve >99% densification from hot pressing, temperatures of 1800–2000 °C and pressures of 30 MPa or greater are required [13]. Spark plasma sintering (SPS) often relies on slightly lower temperatures and significantly reduced processing times compared to hot pressing. During SPS, a pulsed direct current passes through graphite dies with uniaxial pressure exerted on the sample. Grain growth is suppressed by rapid heating over the range 1500–1900°C; this minimizes the time the material has to coarsen [14,15]. Higher densities, cleaner grain boundaries, and elimination of surface impurities can all be achieved by SPS. Most of the UHTC composites can be prepared with 99% density at 2000°C in 5 mins via SPS [16].

**TABLE 1.** Selected properties of some UHTCs [3-5].

Material	Crystal structure	Density (g/cm <sup>3</sup> )	Melting Point (°C)
TaC	Cubic	14.50	3800
TaB <sub>2</sub>	Hexagonal	12.54	3040
TaN	Cubic	14.30	2700
HfC	FCC	12.76	3900
HfB <sub>2</sub>	Hexagonal	11.19	3380
HfN	FCC	13.9	3385
ZrC	FCC	6.56	3400
ZrB <sub>2</sub>	Hexagonal	6.10	3245
ZrN	FCC	7.29	2950

The aim of this research is to develop the nearly full dense composites from TaC and HfC in the vol.% ratio of 80/20 and the effect of MoSi<sub>2</sub> and CNTs on sintering were investigated. The sintering progress was studied base on physical/mechanical and phase/microstructural analysis.

## 2. MATERIALS AND METHOD

Available commercial TaC (d<sub>0.5</sub>=1-2 μm, Treibacher, Austria), HfC (d<sub>0.5</sub>=0.5-0.8 μm, Treibacher, Austria), MoSi<sub>2</sub> (d<sub>0.5</sub>=2-3 μm, ABCR, Germany) and MWCNTs (99.5% purity, 20-50 nm dia., Hodogaya, Japan) were used as starting material. The samples were prepared according to Table 2. All of the materials were mixed in a PTFE jar mill using ethanol and 5 mm SiC balls for 24 h. For CNT containing samples, the CNTs were dispersed using sodium dodecyl sulphate SDS (Merck AG, Germany) in ethanol followed by ultra sonication process. The CNTs containing solution was added to the

other raw materials in jar mill. The mixtures were dried in rotary evaporator under vacuum and passed through - 60 mesh sieve. The specimens were sintered by means of SPS (FCT HP D25/1) at 2000°C under vacuum in a 20 mm graphite die. The heating rate, soaking time and applied pressure during SPS were 100°C/min, 5 mins and 50 MPa, respectively.

**TABLE 2.** Batch composition of the samples (Vol.%).

Sample Code	TaC	HfC	MoSi <sub>2</sub>	CNT
TH	80	20	0	0
THM	80	20	10	0
THC	80	20	0	3
THMC	80	20	10	3

The final dimensions of sintered samples were 20 mm in diameter and 4-6 mm thickness. The specimens were sectioned, ground and polished using diamond abrasive discs. Density of the samples was measured by Archimedes technique (ASTM C830-93). Theoretical densities were calculated based on the mixtures rule. The theoretical densities of TaC, HfC, MoSi<sub>2</sub> and CNTs were considered equal to 14.5, 12.6, 6.3 and 22, respectively. The hardness (HV<sub>10</sub>) measurements were performed by indentation method (Universal Emco-test M1C 010 micro-hardness system, Austria) under 10 kg load and 10 s dwell time (DIN EN ISO 6507-2). The indentation fracture toughness (K<sub>IC</sub>) values were examined through the measurement of the diagonal crack lengths based on Anstis method according to equation 1 [17]:

$$K_{IC} = 0.016 \left( \frac{E}{HV} \right)^{1/2} \left( \frac{P}{C^{3/2}} \right) \quad (1)$$

Where HV is the Vickers hardness, P is the applied load and C is half of the crack length. Both hardness and fracture toughness values were measured for at least 5 points for each sample.

The surface characteristic of CNTs was studied using FTIR spectroscopy (Shimadzu IR Solution 8400S, Japan). The structural changes of CNTs before and after sintering was followed by means of Raman spectroscopy (SENTERRA 2009, Germany) equipped with 758 nm Laser source and CCD detector in the range of 500-3500 cm<sup>-1</sup>. Phase identification were conducted by means of X-ray diffractometry (Rigaku Rint 2200, Japan) using X-ray generator equipped with a Ni-filtered Cu lamp (K<sub>α</sub> radiation of 1.5418 Å wavelength) operating at 40 kV and 30 mA. The XRD system was previously calibrated using pure Si reference sample. The X-ray spectra were measured at the step size of 0.04, time per step of 1 s in the 2θ range of 20-80 degree. Polished and fractured surfaces of the

samples were examined by means of scanning electron microscopy (FESEM, Supra 50 VP, Zeiss, Germany).

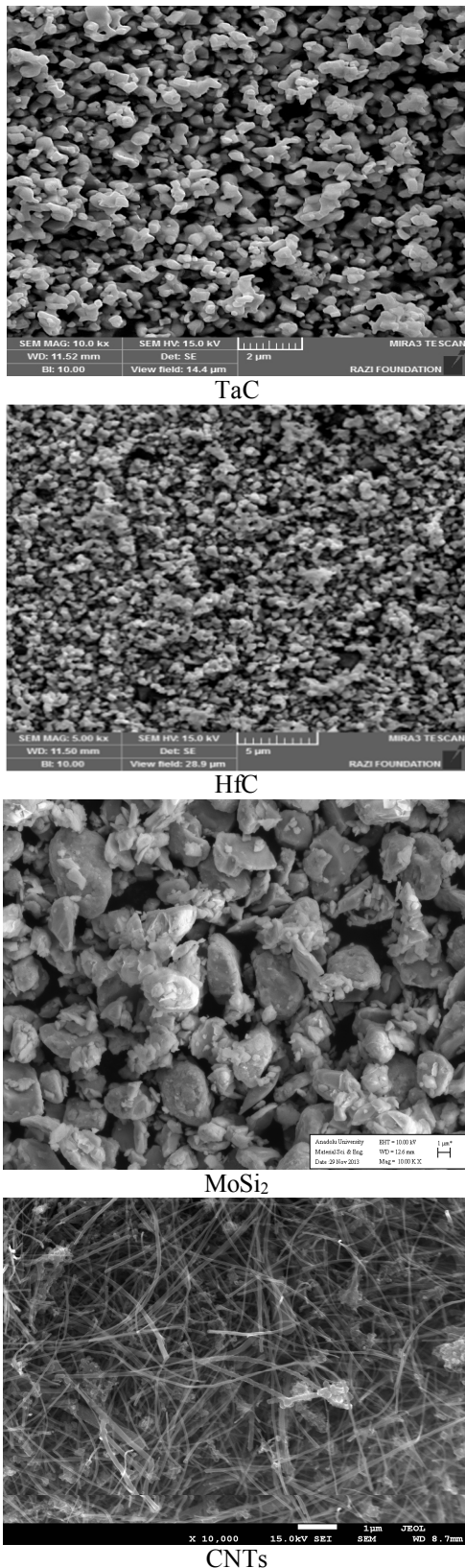


Figure 1. Scanning electron images of used raw materials.

Figure 1. shows the SEM morphology of the used raw materials in this work. As it is shown in this figure, the main TaC, HfC and MoSi<sub>2</sub> powders have submicron sized and angular fine grains. The CNTs are also in the form of agglomerates, should be dispersed in a proper way to be usable as composite reinforcements.

### 3. RESULTS AND DISCUSSION

Figure 2. shows the Raman spectra of the as-received CNTs which proves the presence of the -CH and -OH functional bonds on the external surface of the CNTs walls. This functionalized surface of the CNT product made it very well dispersible during applied batch preparation processing based on the wet mixing method using ethanol liquid media and SDS as organic special dispersant. Dispersion properties of the CNTs are strongly related to the surface charges and the type of the used media in addition to the applied mixing technology in ceramic composite containing CNTs [7]. Table 3 shows the physical and mechanical properties of the spark plasma sintered samples. For TH sample which had no sintering aid, the relative density hardly surpassed 94 % TD, while for CNTs containing one (THC) it reached to 97.2 TD. It is known that the presence of carbonaceous materials enhance the densification properties of UHTCs and especially high temperature carbide materials [18-20].

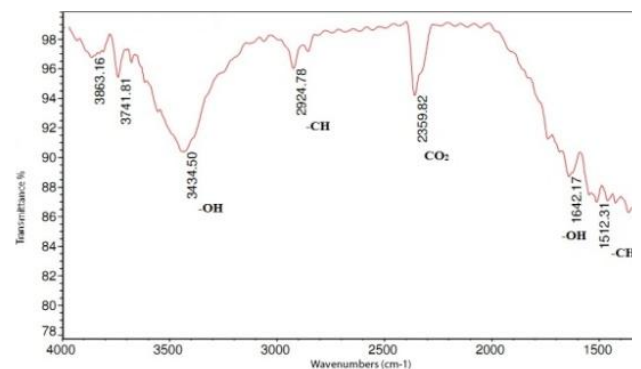


Figure 2. FTIR spectroscopy of as-received CNTs.

The densification results prove the efficiency of MoSi<sub>2</sub> as sintering aid on the sintering behavior of the materials. For THM and THMC samples which contain 10 Vol.% MoSi<sub>2</sub>, the relative density values reached to 99.8 and 98.1 %TD, respectively, after spark plasma sintering at 2000 °C, 50 MPa and 5 min soaking time. In general, MoSi<sub>2</sub> acts as a potentially good liquid phase-assisted sintering aid for refractory carbides and mainly inhibits grain growth and enhances oxidation resistance. Formation of silicide based liquid phase around carbide grains will be conducted at temperature above 1700 °C [11]. MoSi<sub>2</sub> can also enhance the generation of the

diffusion paths for mass transfer which leading to better consolidation of refractory carbides at 1800 °C [12]. The mechanical properties are also in agreement with the densification results obtained for spark plasma sintered samples. By more completion of the densification, higher values of hardness and fractured toughness were obtained. For THMC samples which contains both MoSi<sub>2</sub> and CNTs as reinforcement, the values of 5.3 MPa.m<sup>1/2</sup> achieved for fractured toughness which is attributed to the well densification (because of using 10Vol.% MoSi<sub>2</sub>) and activation of CNTs pull out mechanism [8].

**TABLE 3.** Physical/mechanical properties of the samples.

Sample Code	Relative Density%	HV <sub>10</sub> (GPa)	K <sub>IC</sub> (MPa.m <sup>1/2</sup> )
TH	94.2	16.3±0.2	2.9±0.1
THM	99.8	18.5±0.5	4.2±0.2
THC	97.2	17.8±0.5	4±0.3
THMC	98.1	19.9±0.2	5.3±0.6

(± shows standard deviation.)

Figure 3. shows the X-ray diffraction patterns of raw carbide materials in addition to the spark plasma sintered samples. Both TaC and HfC materials have very similar crystal structure and lattice parameters resulting in the same XRD spectra with some differences in the peak positions. As it is expected, after spark plasma sintering and consolidation of materials, the solid solution phase were produced and TaC grains taking part into the reaction with HfC grains. For MoSi<sub>2</sub>containing samples, the formation of solid solution is proved to be done completely and there is no evidence of any other solid solution peaks in the XRD patterns of THM and THMC samples. While for TH and THC samples (which had no MoSi<sub>2</sub> content), the presence of another minor solid solution phase is clear. It is expected that this minor phase was formed due to the diffusion of Ta in the HfC grains. So, in spite of the formation of major solid solution phase in the Sped composites which was TaC-rich (TaC<sub>ss</sub>), this minor solid solution phase is HfC-rich (HfC<sub>ss</sub>) and its peaks are near to the main HfC peaks position. While for TaC<sub>ss</sub> phase, the positions of the peaks are clearly closed to the host TaC ones.

As described before, 4:1 mole ratio tantalum hafnium carbide solid solution phase has the highest melting point among all refractory ceramics with a general formula Ta<sub>x</sub>Hf<sub>1-x</sub>C<sub>y</sub>. These two materials individually have the highest melting points of 3983 and 3928 °C, respectively, and binary Ta<sub>4</sub>HfC<sub>5</sub> solid solution have a melting point of 4215°C [21,22]. In our previous study [23], the properties of the spark plasma sintered samples containing diverse amounts of MoSi<sub>2</sub> sintered at 1800

°C with the similar conditions were investigated. According to the obtained XRD results, the presence of these both TaC and HfC-rich solid solution phases were proved. In compare to the results obtained in this work, it is demonstrated that, in addition to the usage of sintering aid even at higher volume percentages, the higher SPS soaking temperature is also needed to fulfill the solid phase formation during sintering in this system. Figure 4. shows the Raman spectroscopy results of the as-received CNTs in compare to the spark plasma sintered THMC sample which having MoSi<sub>2</sub> as sintering aid. As it is expected, the positions of D and G bonds show Id/Ig (D to G bond intensity ratio) for both as-received CNTs and THMC sample.

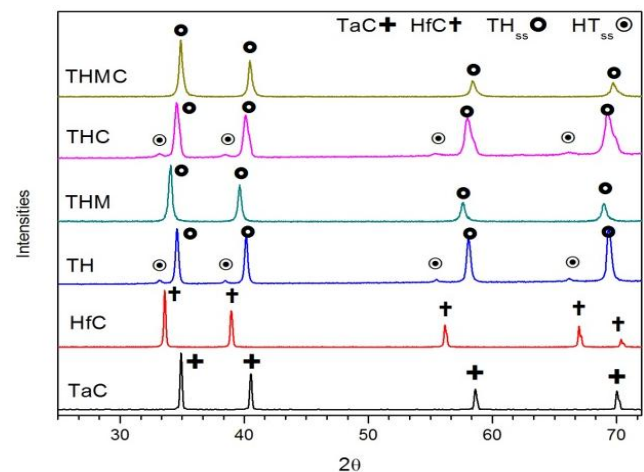


**Figure 3.** X-ray diffraction patterns of the raw carbide materials and the SPS sintered samples.

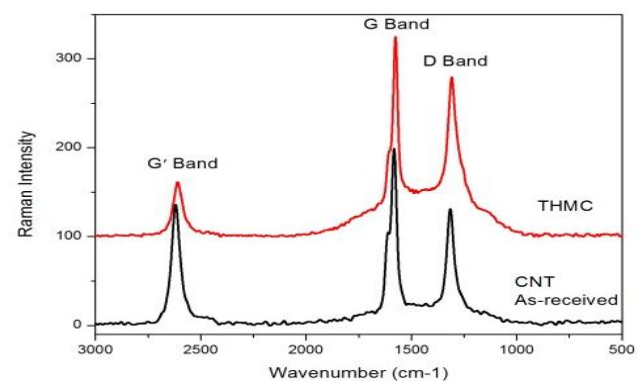


**Figure 4.** RAMAN spectroscopy graphs of the as-received CNTs and THMC SPS sintered sample.

This proves that no significant structural damages were happened to the CNTs during spark plasma processing. There are lots of debates on the structural changes of the CNTs in the ceramic matrix composites containing CNTs which happens during processing especially at high temperature and high pressure conditions [7]. It

is proposed that, during SPS processing, because of the fast heating rate of the sintering, the CNTs don't suffer too much structural changes under high temperature and pressure. Bakhshi et al [14] declared the small  $I_d/I_g$  ratio changes of CNTs in TaC based samples containing 3 wt.% CNTs which were spark plasma sintered at different temperature and applied external loads. Temperature and pressure are normally assumed as external factors which may affect CNTs structure in composites. Other important sources of damages are those ones caused by possible reactions between CNTs and matrix grains. According to Fan et al studies [24], the carbon may react with  $MoSi_2$  at high temperature to form molybdenum carbides. However, according to the XRD and Raman spectroscopy results, there was not any trace of this compound in the phase analysis of THMC sample which had both  $MoSi_2$  and CNTs with together. This result is in a good agreement with Raman spectroscopy analysis of this sample which showed the presence of any structural damage of the CNTs. It seems that the kinetic condition for reaction of  $MoSi_2$  with CNTs is not provided and this would happen because of very high speed heating rate of SPS process (100 °C/min.).

Figures 5(a) and 3(b) show the SEM images of fracture surfaces of THM and THMC spark plasma sintered samples. It can be seen that the sizes of all grains are less than 5  $\mu m$  and there is not any exaggerated grain growth. In the CNTs containing sample (THMC), well dispersion of CNTs in the composite obtained and clear CNTs agglomerates or bundles are not visible. This evidence proves the survivability of CNTs after SPS processing and hence they would act as toughening reinforcement in the texture to enhance the fracture toughness via pull out mechanism. Figure 6 shows the SEM image of a crack path in THMC samples after indentation test. As it is shown, the presence of melted  $MoSi_2$  (gray phase) and some secondary formed SiC particles (Black phase) enabled the matrix to deflect the cracks and increase the fracture toughness values for this sample. Bakhshi et al. reported the enhanced densification and grain growth inhibition effects of CNTs in spark plasma sintered TaC bodies at 1850 °C, 100, 250 and 330 MPa and 10 mins holding time. It can be concluded that carbon nanotubes are potentially attractive as high performance nanoscale reinforcement in ultra high temperature ceramic carbides, including  $MoSi_2$  containing systems, due to their extremely high stiffness and high strength. The incensement in mechanical properties in terms of fracture toughness has been previously reported in diverse kinds of polymer, metal and ceramic matrix composites containing CNTs.

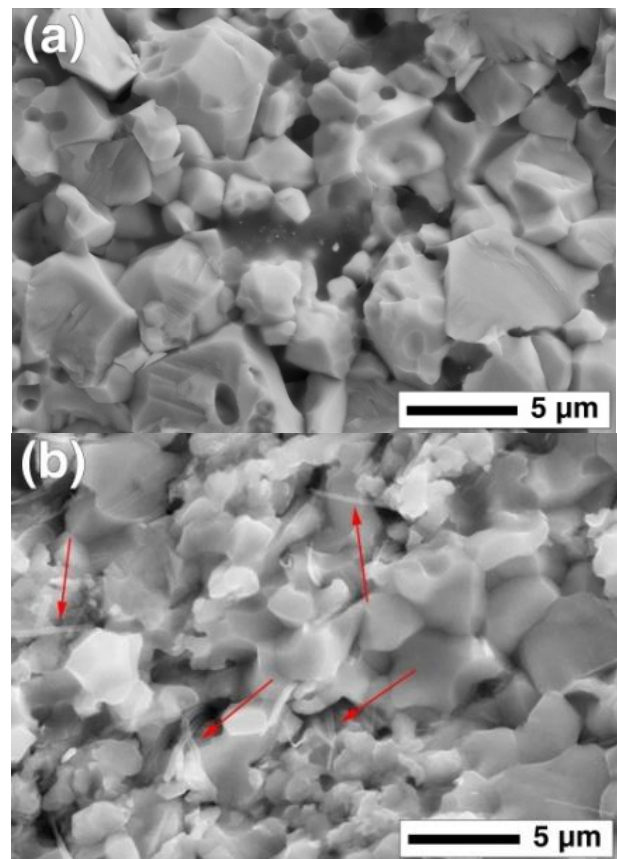


**Figure 5.** SEM fracto-micrographs of the SPS sintered (a) THM and (b) THMC samples.

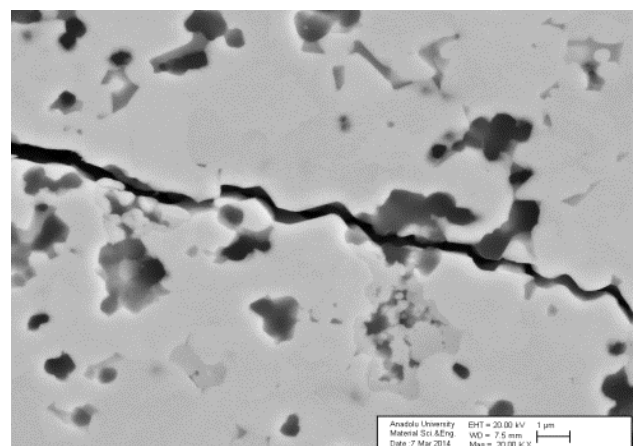


**Figure 6.** SEM image of a crack path in THMC samples after indentation test.

#### 4. CONCLUSION

- High density, mono phase Ta<sub>4</sub>HfC<sub>5</sub> based composites were fabricated by means of spark plasma sintering of TaC and HfC materials using MoSi<sub>2</sub> at 2000°C for 5 mins under 50 MPa pressure.
- The fabricated Ta<sub>4</sub>HfC<sub>5</sub> sample doped by MoSi<sub>2</sub> had density values more than 99% and average Vickers hardness and fracture toughness of 18.5 GPa and 4.2 MPa.m<sup>1/2</sup>, respectively. By combination of CNTs as reinforcement the average Vickers hardness and fracture toughness of 19.9 GPa and 5.3 MPa.m<sup>1/2</sup>, were achieved.
- Regarding the fracto-micrography and Raman spectroscopy studies, the CNTs are well survived in the sample after spark plasma sintering at 2000 °C.
- Regarding the densification and microstructural investigations, it was found that MoSi<sub>2</sub> enhances liquid phase assisted mechanism during intermediate stage of sintering which finally promotes the sintering behavior of the samples.
- It seems that the increase of fracture toughness of CNTs containing samples is due to the activated bridging and pulls out mechanisms.

#### ACKNOWLEDGMENTS

The authors would like to thank to Anadolu University in Turkey for providing some of the used facilities in this work.

#### REFERENCES

1. Kim B.R., Woo K.D., Doh J.M. , Yoon J.K., Shon I.J., "Mechanical properties and rapid consolidation of binderless nanostructured tantalum carbide", *Ceramics International* Vol. 35, (2009) 3395-3400.
2. Silvestroni L., Sciti D., "Sintering Behavior, Microstructure, and Mechanical Properties: A Comparison among Pressureless Sintered Ultra-Refractory Carbides", *Advances in Materials Science and Engineering*, (2010) 1-11.
3. Silvestroni L., Sciti D., Kling J., Lauterbach S., Kleebe H.J., "Sintering Mechanisms of Zirconium and Hafnium Carbides Doped with MoSi<sub>2</sub>", *Journal of American Ceramic Society*, Vol. 92, No. 7, (2009) 1574-1579.
4. Morris R.A. , Wang B. , Matson L.E. , Thompson G.B. , "Microstructural formations and phase transformation pathways in hot pressed tantalum carbides", *Acta Materialia* Vol. 60, No. 1, (2012) 139-148.
5. Chen W., Anselmi-Tamburini U., Garay J.E., Groza J.R., Munir Z.A., "Fundamental investigations on the spark plasma sintering synthesis process I. Effect of dc pulsing on reactivity", *Materials Science and Engineering A*, No. 394, (2005) 132-138.
6. Khaleghi E., Lin Y.Sh., Meyers M.A. , Olevsky E.A. , "Spark plasma sintering of tantalum carbide", *Scripta Materialia*, Vol. 63, No. 6, (2010) 577-580.
7. Li W., Olevsky E.A., McKittrick J., Maximenko A.L., German R.M., "Densification mechanisms of spark plasma sintering: multi-step pressure dilatometry", *Journal of Material Science*, DOI 10.1007/s10853-012-6515-y, (2012).
8. Anstis G.R., Chantikul P., Lawn B.R., Marshall D.B. "A critical evaluation of indentation techniques for measuring fracture toughness: I. Direct crack measurements". *Journal of the American Ceramic Society*, Vol. 64, No. 9, (1981) 533-8.
9. Zhang X., Hilmas G.E. , Fahrenholtz W.G. , "Densification and mechanical properties of TaC-based ceramics", *Materials Science and Engineering: A* Vol. 501, No. 1-2, 15 (2009) 37-43.
10. Bakshi S.R., Musaramthota V., Virzi D.A., Keshri A.K., Lahiri D., Singh V., Seal S., Agarwal A., "Spark plasma sintered tantalum carbide: effect of pressure and carbon nanotube addition on microstructure and mechanical properties", *Materials Science and Engineering A*, Vol. 528, (2011) 2538-47.
11. Lahiri D., Khaleghi E. , Bakshi S. R. , Li W. , Olevsky E.A. , Agarwal A., "Graphene-induced strengthening in spark plasma sintered tantalum carbide-nanotube composite", *Scripta Materialia* Vol. 68, No. 5, March, (2013) 285-288.
12. Gusev A.I., "Phase Diagram of the Pseudo-binary TiC-NbC, TiC-TaC, ZrC-NbC, ZrC-TaC and HfC-TaC Carbide Systems", *Russian Journal of Physical Chemistry*, Vol. 59, No. 3, (1985) 35-42.
13. Nazarova S.Z. , Kurmaev E.Z. , N. I. Medvedeva, Mowes A. , "Physical properties and electronic structure of TaC-HfC solid solutions", *Russian Journal of Inorganic Chemistry*, Vol. 52, No. 2, (2007) 233-237.
14. Arianpour F., Rezaie H.R., Golestani Fard F., Fantozzi G., Mazaheri M., "Processing and Consolidation of TaC/HfC Based Composites Using MoSi<sub>2</sub> and Carbon Nanotubes", *Journal of Nano Research*, Vol. 21 (2013) 145-150.
15. Fan X., Hack K., Ishigaki T., "Calculated C-MoSi<sub>2</sub> and B-Mo<sub>5</sub>Si<sub>3</sub> pseudo-binary phase diagrams for the use in advanced materials processing", *Materials Science and Engineering A*, Vol. 278 (2000) 46-53.